Transport through a single donor in p-type silicon

J. A. Miwa,[1] J. A. Mol,[1,2] J. Salfi,[1] S. Rogge,[1] and M. Y. Simmons[1,a)]
[1]*Centre of Excellence for Quantum Computation and Communication Technology, University of New South Wales, Sydney, NSW 2052, Australia*
[2]*Kavli Institute of Nanoscience, Delft University of Technology, Lorentzweg 1, 2628 CJ Delft, The Netherlands*

(Received 27 May 2013; accepted 5 July 2013; published online 23 July 2013)

Single phosphorus donors in silicon are promising candidates as qubits in the solid state. Here, we present low temperature scanning probe microscopy and spectroscopy measurements of individual phosphorus dopants deliberately placed in p-type silicon ~1 nm below the surface. The ability to image individual dopants combined with scanning tunnelling spectroscopy allows us to directly study the transport mechanism through the donor. We show that for a single P donor, transport is dominated by a minority carrier recombination process with the surrounding p-type matrix. The understanding gained will underpin future studies of atomically precise mapping of donor-donor interactions in silicon. © *2013 AIP Publishing LLC*. [http://dx.doi.org/10.1063/1.4816439]

Understanding electron transport through solitary dopants in silicon is important for both commercial devices and new applications in the area of quantum information or single-dopant transistors.[1,2] In particular, as commercial devices reach the atomic limit in size,[1–8] device characteristics become dominated by transport through a single dopant impurity.[9] A consequence of reduced device dimensions is that the majority of dopants will reside in the vicinity of an interface, where their properties are known to change. For example, enhanced binding energies for impurities nearer to a surface have been reported[7,10–13] and pronounced changes in the spatial extent of the impurity wavefunction as a function of depth have been observed.[14–18] Such changes in the character of these impurities can have profound affects on device performance. For these reasons, fundamental studies about the behaviour of individual impurities in semiconductors have recently garnered much attention.[14,19,20] A scanning tunnelling microscope (STM) is an ideal tool to investigate such systems because it provides the location of the addressed impurity with atomic accuracy,[10] and more importantly, it can acquire transport data through the impurity. Combined, this information will provide us with unique information on the influence of the local electronic environment on the properties of individual impurities.[16]

In this letter, we investigate the electronic properties of single phosphorus donors in a p-type (boron) silicon host matrix buried nominally 1 nm below the (001) surface. This material system is technologically relevant for recent developments in donor based quantum computing architectures, where individual donors are placed in silicon with atomic precision using a scanning tunnelling microscope with phosphine (PH_3) and epitaxial silicon overgrowth.[2,6,21] Epitaxial overgrowth allows us to encapsulate the donors at a given depth, which are then imaged by the microscope. The extent to which impurities can be buried and still imaged by STM depends on several factors, such as the Bohr radius of the impurity, the surface quality of the silicon encapsulation, the tip work function and the extent of tip induced band bending. Previously, we have demonstrated that we can image P donors buried under 1 nm of n-type silicon.[22,23] Here, we employ scanning tunnelling spectroscopy (STS) measurements at 77 K to locally probe minority carrier recombination for electrons of a single donor to the p-type substrate. From detailed spectroscopy measurements, we extract a carrier lifetime of 4 ns which is limited by the presence of the nearby surface. Ultimately, these measurements establish that cryogenic STS can be applied to *in situ* grown, buried dopant structures, and that carrier recombination can be probed at the single dopant level. Moreover, we form the foundations that will allow us to directly assess the performance of multi-donor devices.

STM and STS measurements were performed with an Omicron low temperature STM (LT-STM) with a base pressure of 1×10^{-11} mbar. A schematic of the doping process is illustrated in Figure 1(a). After flashing a boron doped (8×10^{18} cm^{-3}) sample to reconstruct the surface to 2×1 (Figure (a-I)), the sample is exposed to 0.02 Langmuir of PH_3 gas (Figure (a-II)) and gently heated to approximately 600 °C for 60 s to incorporate P atoms into the top layer of the surface.[24] The sample is held at room temperature to suppress dopant segregation and approximately 1 nm of epitaxial Si is grown at a rate of 0.26 Å/h (Figure (a-III)). Following encapsulation with epitaxial silicon, the sample was annealed to 450 °C for 5 s to promote a smooth surface for imaging. P donor diffusion is expected to be minimal during the rapid anneal due to a high P diffusion energy barrier of 3.66 eV within the bulk.[25] The estimated carrier density is 2.4×10^{12} cm^{-2} resulting in a sparse distribution of P donors in which donor-donor interactions can be excluded.

Hydrogen-passivation (depicted in Figure (a-IV)) is known to preserve the 2×1 morphology of the clean Si(001) surface,[26] but has a featureless band gap, allowing the buried donors to be measured directly by STM/STS.[27] Depending on the polarity of the applied sample bias, the buried donors manifest as either dark depressions or bright protrusions superimposed on the dimer rows of the surface as shown in Figure 1(b). To understand this bias dependence, the schematic in Figure 2 (left) describes the tunnelling process that occurs for filled state imaging, where applying a negative sample bias,

a)Electronic mail: michelle.simmons@unsw.edu.au

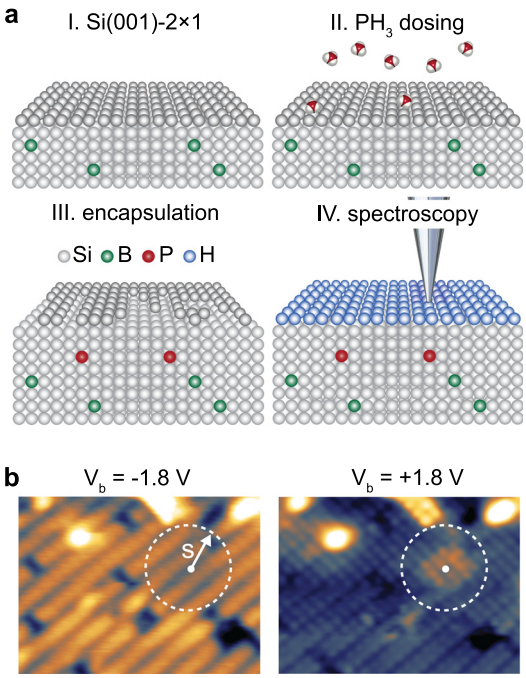

FIG. 1. Imaging single P dopants prepared by a monolayer doping process. (a) Schematic of monolayer doping process: (I) A Si(001) surface is flashed to high temperatures to promote a 2×1 surface reconstruction. (II) The surface is then dosed with phosphine gas which adsorbs to the highly reactive Si surface and dissociates before being heated to ~600 °C to incorporate P dopants into the surface. (III) The dopants are then encapsulated with epitaxial Si grown by low temperature silicon molecular beam epitaxy. (IV) The surface is passivated with atomic hydrogen to allow imaging of the buried donors by scanning tunneling microscopy. (b) In filled state images (negative sample bias), the buried P donor appears as a dark depression superimposed on the atomically resolved silicon surface. The lateral tip displacement with respect to the donor nucleus s is indicated with an arrow, the position of the donor nucleus is indicated with a dot. In empty state images, the donor appears as a bright protrusion extending ≈2 nm in diameter. Imaging parameters: $V = \pm 1.8$ V, $I = 0.3$ nA, and 18×13 nm^2.

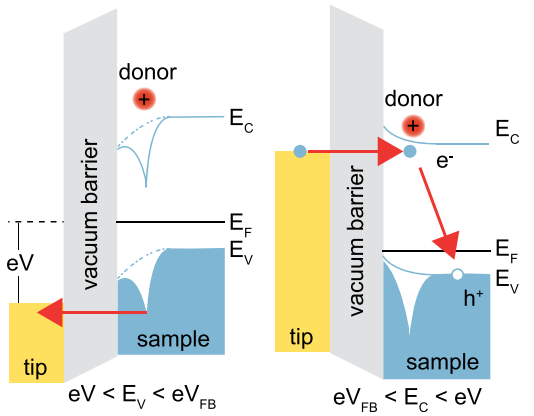

FIG. 2. Tunneling processes through individual buried P donors in p-type silicon. (Left) Schematic of the tunneling process through a buried P donor in a p-type substrate for filled state imaging. (Right) Schematic representation of resonant hole transport through the localized state of a buried acceptor at high positive bias in empty state imaging. Here, an electron tunnels from the tip into the localized donor state where transport is Coulomb blocked until the donor-bound electron recombines with a hole in the valence band. As a consequence, the current is limited by the electron-hole recombination rate. V_{FB} denotes the flat-band voltage.

V such that eV $<$ E_V-E_F (where E_V is the valence band edge and E_F is the sample Fermi level) results in electrons tunneling from the valence band to the tip (see red arrow). The resulting positively charged nucleus of the buried donor leads to a decrease in the local density of states (LDOS) and appears as a broad depression superimposed on the dimer rows of the silicon surface. The decrease in height in filled state imaging varies slowly since it results from repulsive scattering of free carriers from the ionized donor thereby closely reflecting the Coulomb potential of the donor. Conversely, when a positive voltage greater than the conduction band minimum is applied (eV $>$ E_C-E_F) there is an increase in the tunneling current to the conduction band near the donor. The buried donors therefore appear as a bright protrusion superimposed on the dimer rows in empty state images (Figure 1(b), right image). The increase in current, and as a consequence tip height, is abrupt and localized since it arises from direct tunneling into the localized donor state where we directly image the donor wavefunction. Similar effects have been observed for buried donors,[28–30] and a complimentary effect reported for buried acceptors.[29,31–33] We note that buried P donors have been observed on the Si(111)-2×1 reconstructed surface, in which a bias dependent contrast is observed due to dopant incorporation at inequivalent lattice sites in the uppermost layers of the reconstructed surface.[31] Such bias dependent contrast is not observed in the Si(001)-2×1 surface since lattice sites for P incorporation are equivalent.

STS allows us to gain information on both the energetic and spatial dependence of the LDOS.[34] From the individual I-V traces, we can construct the conductance map shown in Figure 3(a), where the normalized conductance, $g_N = (dI/dV)/(I/V)$, is plotted as function of applied sample bias (V) and position (x). Regions in yellow (white) correspond to areas of low (high) conductance on the color scale. The buried P donor appears laterally at $x \approx 2.1$ nm. We observe a Coulombic downward shift of the valence band due to the ionized donor's Coulomb potential and resonant tunnelling into a localized state below the conduction band edge E_C. In Figure 3(b), we show the normalized conductance measured directly above the donor (solid blue curve) and away from the donor (dashed green curve). We can quantify the changes in the onset of both the valence (ΔV_V) and conduction (ΔV_C) band edges by determining the slopes (dotted red lines) of individual normalized conductance curves.[34] The difference in slope provides a direct measure of the effect of the buried donor on the LDOS. The onset of tunnelling into the P donor induced state below the conduction band is abrupt since tunnelling into the localized state induces a single level independent of the tip position.[28,35] However, the valence band shift exhibits a clear Coulombic nature as expected since the shift arises from valence band states scattering from the repulsive positively charged nucleus of the donor.[28] From this shift, we can directly determine the depth of the buried donor by fitting to a Coulomb potential[33]

$$\Delta E_V \approx e \frac{e - Q}{4\pi\epsilon_0\epsilon_{Si}} \frac{1}{\sqrt{s^2 + d^2}}, \quad (1)$$

where $Q = e(\epsilon_v - \epsilon_{Si})/(\epsilon_v + \epsilon_{Si})$ is the image charge due to the mismatch between the dielectric constants ϵ_v and ϵ_{Si} of the vacuum and silicon, respectively, and s is the lateral separation between the tip apex and the donor nucleus along the interface (see Figure 1(b)). We performed this analysis for

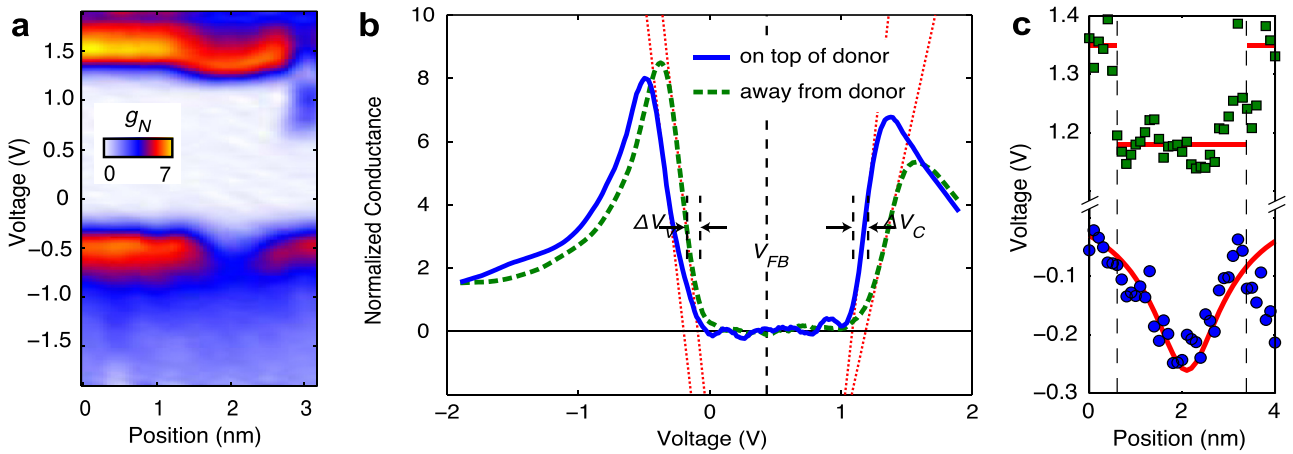

FIG. 3. Spectroscopy of a single P donor. (a) False color map of the normalized conductance as a function of applied sample bias and position compiled from I-V curves acquired while simultaneously recording occupied state images. (b) Two normalized conductance curves are presented: one acquired directly above the buried donor (solid blue line) and one away from the donor (dashed green line). The edges of the valence and conduction bands are defined by the slopes (red dashed lines) of the normalized conductance at a position away from the buried donor. A clear shift in both the valence and conduction bands is observed. (c) Plot of the measured valence band (solid blue dots) and conduction band (solid green squares) shift as a function of position across the buried donor. The fit (red solid lines) to the valence band shift exhibits a clear Coulomb potential and the conduction band shift shows a distinct localized state character.

several buried donors and from these determined the average depth of the donor, $d = 0.70 \pm 0.04$ nm. Considering the degree of donor segregation expected for the growth conditions used this agrees well with the expected encapsulation depth of approximately 1 nm.[23] This result highlights the use of a simple electrostatic approach to effectively model our system using static dielectric and image charges.

Since a relatively small density of P donors were placed in a heavily doped (8×10^{18} cm^{-3}) p-type substrate, the majority carriers are holes. In thermal equilibrium, the P dopants will be compensated by the heavily boron doped sample and all the P donors will be ionized. If we now consider resonant transport through the localized donor state, it will be sequential where only one electron can occupy the donor at each given moment. However, at high positive bias, any minority carriers (electrons) that are injected from the tip will need to recombine with holes in the valence band in order for the next electron to tunnel onto the donor. This is a consequence of the donor level being below the conduction band edge such that electrons cannot tunnel from the donor into the conduction band (Figure 2(b)). As long as an electron resides on the donor, transport is Coulomb blocked.[36]

The absence of a Coulombic feature in the conduction band (Figure 3(c)), therefore, indicates that at positive bias the donor is neutral.[28] Each time a localized electron recombines with holes from the valence band, another electron is rapidly loaded from the tip. The tunnelling current, $I = e\Gamma_{in}\Gamma_{out}/(e\Gamma_{in} + \Gamma_{out})$, is determined by the tunnel rate from the tip to the donor (Γ_{in}) and the recombination rate, $\Gamma_{out} = 1/\tau$, where τ is the carrier lifetime. If $\Gamma_{in} \gg \Gamma_{out}$, the tunnelling current $I = e\Gamma_{out} = e/\tau$ will be dominated by the carrier lifetime. From the tunnel current through the localized state, we obtain a carrier lifetime of $\sim$4 ns. This is a striking result as it is two orders of magnitude lower than that reported for phosphorus in bulk silicon.[37] We can however attribute the suppression in carrier lifetime to additional recombination channels provided by the nearby surface which as well as being hydrogen terminated likely contains imperfections in the overgrown layer.

In summary, using STS, we have measured electron transport through a single P donor buried nominally 1 nm below the silicon surface in a p-type matrix. These buried dopants were prepared using a gaseous dopant source in combination with epitaxial silicon overgrowth, the same process recently used to fabricate a precision single atom transistor.[2] Using a simple electrostatic model, we independently confirm the placement of P donors 1 nm below the surface. Importantly, we show that under positive bias transport occurs via a recombination process with holes from the valence band. We directly measure a carrier lifetime of $\approx$4 ns which was found to be limited by the minority carrier recombination rate due to donors being so close to the surface. The ability to image wavefunctions and perform quantitative transport measurements on future STM-patterned dopants will pave the way towards spatially resolved, atomically precise mapping of quantum transport in multi-donor devices.

This research was conducted by the Australian Research Council Centre of Excellence for Quantum Computation and Communication Technology (Project No. CE110001027) and the U.S. National Security Agency and the U.S. Army Research Office under Contract No. W911NF-13-1-0024. M.Y.S. acknowledges an ARC Federation Fellowship.

[1]P. M. Koenraad and M. E. Flatté, Nature Mater. **10**, 91 (2011).
[2]M. Fuechsle, J. A. Miwa, S. Mahapatra, H. Ryu, S. Lee, O. Warschkow, L. C. L. Hollenberg, G. Klimeck, and M. Y. Simmons, Nat. Nanotechnol. **7**, 242 (2012).
[3]K. Y. Tan, K. W. Chan, M. Mottonen, A. Morello, C. Yang, J. v. Donkelaar, A. Alves, J.-M. Pirkkalainen, D. N. Jamieson, R. G. Clark, and A. S. Dzurak, Nano Lett. **10**, 11 (2010).
[4]M. Pierre, R. Wacquez, X. Jehl, M. Sanquer, M. Vinet, and O. Cueto, Nat. Nanotechnol. **5**, 133 (2010).
[5]L. Calvet, J. Snyder, and W. Wernsdorfer, Phys. Rev. B **78**, 195309 (2008).
[6]B. Weber, S. Mahapatra, H. Ryu, S. Lee, A. Fuhrer, T. C. G. Reusch, D. L. Thompson, W. C. T. Lee, G. Klimeck, L. C. L. Hollenberg, and M. Y. Simmons, Science **335**, 64 (2012).
[7]G. Lansbergen, R. Rahman, C. Wellard, I. Woo, J. Caro, N. Collaert, S. Biesemans, G. Klimeck, L. Hollenberg, and S. Rogge, Nat. Phys. **4**, 656 (2008).

[8]A. Morello, J. J. Pla, F. A. Zwanenburg, K. W. Chan, K. Y. Tan, H. Huebl, M. Mottonen, C. D. Nugroho, C. Yang, J. A. van Donkelaar, A. D. C. Alves, D. N. Jamieson, C. C. Escott, L. C. L. Hollenberg, R. G. Clark, and A. S. Dzurak, Nature **467**, 687 (2010).
[9]S. Roy and A. Asenov, Science **309**, 388 (2005).
[10]A. P. Wijnheijmer, J. K. Garleff, K. Teichmann, M. Wenderoth, S. Loth, R. G. Ulbrich, P. A. Maksym, M. Roy, and P. M. Koenraad, Phys. Rev. Lett. **102**, 166101 (2009).
[11]H. Sellier, G. Lansbergen, J. Caro, S. Rogge, N. Collaert, I. Ferain, M. Jurczak, and S. Biesemans, Phys. Rev. Lett. **97**, 206805 (2006).
[12]S. Perraud, K. Kanisawa, Z.-Z. Wang, and T. Fujisawa, Phys. Rev. Lett. **100**, 056806 (2008).
[13]G. Bastard, *Wave Mechanics Applied to Semiconductor Heterostructures* (Les Editions de Physique, Les Ulis, 1988).
[14]S. Loth, M. Wenderoth, and R. Ulbrich, Phys. Rev. B **77**, 115344 (2008).
[15]F. Marczinowski, J. Wiebe, J.-M. Tang, M. Flatte, F. Meier, M. Morgenstern, and R. Wiesendanger, Phys. Rev. Lett. **99**, 157202 (2007).
[16]J. Garleff, C. Celebi, W. van Roy, J.-M. Tang, M. Flatte, and P. Koenraad, Phys. Rev. B **78**, 075313 (2008).
[17]S. Loth, M. Wenderoth, R. Ulbrich, S. Malzer, and G. Dohler, Phys. Rev. B **76**, 235318 (2007).
[18]C. Celebi, J. K. Garleff, A. Y. Silov, A. M. Yakunin, P. M. Koenraad, J.-M. Tang, and M. E. Flatte, Phys. Rev. Lett. **104**, 086404 (2010).
[19]D. H. Lee and J. A. Gupta, Science **330**, 1807 (2010).
[20]A. M. Yakunin, A. Y. Silov, P. M. Koenraad, J.-M. Tang, M. E. Flatte, J. L. Primus, W. van Roy, J. de Boeck, A. M. Monakhov, K. S. Romanov, I. E. Panaiotti, and N. S. Averkiev, Nature Mater. **6**, 512 (2007).
[21]S. Mahapatra, H. Büch, and M. Y. Simmons, Nano Lett. **11**, 4376 (2011).
[22]L. Oberbeck, N. J. Curson, T. Hallam, M. Y. Simmons, and R. G. Clark, Thin Solid Films **464–465**, 23 (2004).
[23]L. Oberbeck, N. J. Curson, T. Hallam, M. Y. Simmons, G. Bilger, and R. G. Clark, Appl. Phys. Lett. **85**, 1359 (2004).
[24]H. Wilson, O. Warschkow, N. Marks, S. Schofield, N. Curson, P. Smith, M. Radny, D. McKenzie, and M. Simmons, Phys. Rev. Lett. **93**, 226102 (2004).
[25]P. M. Fahey, P. B. Griffin, and J. D. Plummer, Rev. Mod. Phys. **61**, 289 (1989).
[26]J. Boland, Phys. Rev. Lett. **65**, 3325 (1990).
[27]M. C. Hersam, N. P. Guisinger, and J. W. Lyding, Nanotechnology **11**, 70 (2000).
[28]K. Teichmann, M. Wenderoth, S. Loth, R. G. Ulbrich, J. K. Garleff, A. P. Wijnheijmer, and P. M. Koenraad, Phys. Rev. Lett. **101**, 076103 (2008).
[29]L. Liu, J. Yu, and J. W. Lyding, IEEE Trans. Nanotechnol. **1**, 176 (2002).
[30]G. W. Brown, H. Grube, and M. Hawley, Phys. Rev. B **70**, 121301 (2004).
[31]C. Sürgers, M. Wenderoth, K. Löser, J. K. Garleff, R. G. Ulbrich, M. Lukas, and H. von Löhneysen, New J. Phys. **15**, 055009 (2013).
[32]M. Nishizawa, L. Bolotov, and T. Kanayama, Jpn. J. Appl. Phys., Part 2 **44**, L1436 (2005).
[33]J. A. Mol, J. Salfi, J. A. Miwa, M. Y. Simmons, and S. Rogge, Phys. Rev. B **87**, 245417 (2013).
[34]R. Feenstra, Phys. Rev. B **50**, 4561 (1994).
[35]S. Loth, "Atomic scale images of acceptors in III-V semiconductors: Band bending, tunneling paths and wave functions," Ph.D. dissertation (Universitätsverlag Göttingen, 2007).
[36]L. L. Sohn, L. P. Kouwenhoven, and G. Schön, *Mesoscopic Electron Transport* (Springer, 1997).
[37]W. Schmid, Solid-State Electron. **21**, 1285 (1978).